Experimental oscillator strengths in Th II

Nilsson, Hampus; Zhang, Z G; Lundberg, Hans; Johansson, Sveneric; Nordström, Birgitta

Published in:
Astronomy & Astrophysics

DOI:
10.1051/0004-6361:20011597

2002

A&A 382, 368–377 (2002)
DOI: 10.1051/0004-6361:20011597

Astronomy & Astrophysics

Experimental oscillator strengths in Th II

H. Nilsson[1], Z. G. Zhang[2], H. Lundberg[2], S. Johansson[1], and B. Nordström[1,3]

[1] Atomic Astrophysics, Lund Observatory, Lund University, PO Box 43, 22100 Lund, Sweden
[2] Atomic Physics, Department of Physics, Lund Institute of Technology, PO Box 118, 22100 Lund, Sweden
[3] Niels Bohr Institute for Astronomy, Physics & Geophysics, Juliane Marie vej 30, 2100 Copenhagen, Denmark
e-mail: zhang.zhiguo@fysik.lth.se; hans.lundberg@fysik.lth.se; sveneric.johansson@astro.lu.se; birgitta@astro.ku.dk

Received 17 October 2001 / Accepted 5 November 2001

Abstract. We have measured radiative lifetimes of ten Th II levels by using the laser-induced fluorescence technique and branching fractions with Fourier transform spectroscopy. By combining the new branching fractions with a total of 23 lifetimes, from the present work and from measurements by Simonsen et al. (1988), absolute oscillator strengths for 180 lines have been derived. Some of these new f-values reported are relevant for radioactive dating of stars.

Key words. atomic data – stars: evolution – Galaxy: evolution

1. Introduction

One way of estimating the age of the Galaxy is radioactive dating of stars. The idea of such a cosmochronometer is to compare the change with time of the abundance ratio of a radioactive element and a stable element. The present ratio derived from the star's spectrum is compared with the abundance ratio at the formation of the star, predicted from a model. In a recent paper, Cayrel et al. (2001) report the age of a metal deficient star as determined with a uranium-thorium cosmochronometer. The radioactive thorium and uranium isotopes present in the star have half-lifes of 14 Gyr and 4.5 Gyr, respectively. A major part of the uncertainty of the age derived for the star is associated with the oscillator strengths of Th II and U II lines, used in the abundance determinations. This paper deals with f-value data for Th II, which has the ground configuration $6d^2(^3F)7s$. The lowest excited configurations are $5f(^2F)7s^2$ and $5f6d(^3H)7s$.

Oscillator strengths in Th II have been reported by Corliss & Bozman (1962), who measured relative line intensities in an arc spectrum. Corliss (1979) renormalized the intensities using the radiative lifetime of one level measured by Andersen & Petkov (1975). Later Palmer & Engelman (1983) measured relative intensities and accurate wavelengths from a hollow cathode (HC) discharge and normalized the intensities to the gf-values of Corliss & Bozman (1962) by assuming local thermodynamic equilibrium (LTE) in the light source. Simonsen et al. (1988) measured lifetimes for 18 levels in Th II and compared with lifetimes that can be derived from the data presented by Palmer & Engelman (1983). This comparison led Simonsen et al. (1988) to give a formula, which adjusts the gf-values of Corliss (1979). This adjustment results, however, in an inconsistency: The upper limit of the gf-value of λ 4019.1 is 0.63 ($BF = 1$) based on the measured lifetime, whereas the formula gives an adjusted gf-value of 0.79.

In the present paper we present gf-values for 180 Th II lines in the wavelength region 3100–12 600 Å, derived by combining new measurements of both branching fractions (BFs) and radiative lifetimes. For 13 levels we have used the lifetimes measured by Simonsen et al. (1988). The line identifications are taken from the term analysis by Palmer & Engleman (1983).

2. Experiment

2.1. Lifetime measurements

In the present investigation radiative lifetimes of ten levels in Th II were measured using the laser-induced-fluorescence (LIF) technique. A plasma of thorium ions was created by irradiating a thorium target with laser pulses. The measurements were performed close to the target during the expansion of the plasma, in which low-lying metastable levels were populated. The ions were selectively photo-excited to the level under investigation by the light from a pulsed laser system. A Nd:YAG laser pumped a tuneable dye laser, working on a red dye.

Send offprint requests to: H. Nilsson,
e-mail: hampus.nilsson@astro.lu.se

Table 1. Experimental radiative lifetimes of Th II.

Configuration[a]	Energy (cm^{-1})	J	λ^b_{exc} (Å)	λ^c_{obs} (Å)	Exp. Lifetime (ns)[d] this work	S	A&P
$5f(^2F)6d^2(^3F)$	18 214.426	1.5				376(38)	
$5f(^2F)6d^2(^3F)$	19 050.829	1.5				579(58)	
$5f6d(^3D)7s$	19 248.270	2.5				453(45)	
$5f(^2F)6d^2(^3F)$	20 686.146	2.5				502(50)	
$5f6d(^1P)7s$	21 131.799	1.5				1290(323)	
$5f(^2F)6d^2(^3F)$	21 297.416	2.5				315(32)	
$5f(^2F)6d^2(^3F)$	21 682.747	3.5				807(202)	
$5f6d(^1H)7s$	22 642.105	4.5				3560(890)	
$6d7s(^3D)7p$	23 372.581	1.5	4277.314	4277.314	81(5)		
$5f(^2F)6d^2(^3F)$	24 132.035	1.5				159(8)	
$5f(^2F)6d^2(^3F)$	24 414.641	1.5				62.6(1.9)	
$5f(^2F)6d^2(^3F)$	24 463.789	2.5	4086.521	4086.521	95(6)	94.2(3.0)	
$6d7s(^3D)7p$	24 873.983	2.5				23.0(7)	21(3)
$5f(^2F)6d^2(^3P)$	25 188.120	1.5				280(28)	
$5f(^2F)6d^2(^3P)$	25 440.231	2.5	4179.715	3929.669	66(4)	66.2(2.0)	
$5f(^2F)6d^2(^3P)$	26 424.470	2.5	3783.296	3783.296	140(9)	151(8)	
$5f(^2F)6d^2(^3P)$	27 249.544	3.5				125(6)	
$6d7s(^3D)7p$	28 243.812	2.5	3539.587	3741.183	11.5(7)		
$6d7s(^3D)7p$	28 720.835	1.5	3675.567	3721.825	12.5(7)	15.3(5)[e]	
$5f(^2F)6d^2(^1D)$	29 095.464	2.5	3625.628	3435.977	28(2)	29(1)	
$6d^2(^3F)7p$	30 972.162	2.5	3227.774	3433.999	15.5(7)		
$6d7s(^3D)7p$	31 353.125	1.5	3351.228	3351.228	8.8(4)		
$6d^2(^3F)7p$	32 957.429	3.5	3180.194	3469.924	6.5(3)		

[a] Notation according to Blaise & Wyart (1992).
[b] Laser wavelength used to populate the upper state.
[c] Wavelength used to detect the fluorescence signal.
[d] S = Simonsen et al. (1988) (Beam-laser), A&P = Andersen & Petkov (1975) (Beam-foil).
[e] See discussion in the lifetime section.

The dye laser light was shifted to the desired wavelengths in near UV and deep blue using a frequency-doubling crystal and Raman shifting in a hydrogen cell. Fluorescence light released at the decay of the excited levels was captured using a fast detection system. For levels with short lifetimes the temporal shape of the laser pulse was also recorded, and the lifetime values were evaluated by fitting a convolution of the recorded pulse and an exponential to the fluorescence signal. The experimental set-up is described in detail by Li et al. (2000).

For elements having level and line rich spectra selectivity in both excitation and detection is especially important. The band width of the laser light utilized in the present investigation was about 0.1 Å, and the fluorescent light was selected by a monochromator. After setting the laser to the excitation wavelength for a level and observing fluorescence at an expected wavelength, a further test of proper level identification was made by tuning the monochromator to a different decay channel. The lines used for excitation and recording of decay curves are given in Table 1 together with the lifetime values. The excitation wavelengths were taken from Palmer & Engleman (1983). The advantage with a laser produced plasma as ion source is the high ion density, fairly high population in metastable levels and the presence of high ionization stages. A major drawback is the high speed of the created ions, which for singly ionized thorium is in the range 10^3–10^4 m s^{-1}. It sets an upper limit for the lifetime that can be measured due to flight-out-of-view effects (Sikström et al. 2001).

Possible systematic errors due to flight-out-of-view effects were checked by changing the position of the detecting monochromator slit. Another test was to make lifetime recordings for different delays between the ablation laser pulse and the excitation laser pulse, i.e. to perform measurements on ions with different velocities. Our uncertainties are to equal parts given by statistical scattering between different recordings and possible systematic effects.

Five of the levels now studied were included in the beam-laser work of Simonsen et al. (1988). As can be seen in Table 1 the agreement is good for all lifetimes except the shortest one. The energy of this level is given as 28 720.315 cm^{-1} in the work of Simonsen et al. (1988), but there is no known level in Th II at this energy (Blaise & Wyart 1992). The closest level is reported at 28 720.835 cm^{-1}, but there is also one at 29 720.315 cm^{-1}, implying a typo in the table of Simonsen et al. (1988). We measured the lifetimes of both these levels and found the lifetime of 28 720 level to be slightly shorter (12.5 ns) than the value (15.3 ns) reported by Simonsen et al. (1988), and the lifetime of the 29 720 level to be about 70 ns. Our conclusion is that Simonsen et al. (1988) measured the lifetime of the level at 28 720.835 cm^{-1}, and that the deviation from our value might be due to limitations in their measurements.

2.2. Branching fractions

Line intensities have been measured in HC spectra between 2500 and 7000 Å recorded with a Chelsea Instrument FT500 vacuum ultraviolet Fourier transform spectrometer (FTS). The cathode is a 3 cm long cylinder of iron with an inner diameter of 0.5 cm, and the inner wall is covered with a thorium foil. Spectra were recorded at discharge currents between 0.1 and 0.6 A using argon as a carrier gas at a pressure of 0.7 Torr.

The intensities of lines above 7000 Å were obtained from spectra recorded with the FTS at Kitt Peak National Observatory (Palmer & Engleman 1983).

In order to get absolute intensities the spectra had to be corrected for the instrument response. This was done with a tungsten ribbon lamp with known spectral distribution (4100–7000 Å) and Ar II lines with known branching ratios (BR) (2500–5300 Å) (Whaling et al. 1993). For some Th II levels spectra from different recordings had to be combined, and that produces larger uncertainties in the calibration. The uncertainty of the tungsten lamp calibration data is 3%, and the recorded spectrum from the lamp is reproducible within 5%. The uncertainty in the calibration with known BRs of argon is estimated to 10%, and the uncertainty caused by the combination of different spectral regions is estimated to 10%. The spectra from Kitt Peak were intensity calibrated with a tungsten lamp and an argon mini-arc. Palmer & Engleman (1983) claim an uncertainty of 5% in the calibration between 4000–13 500 Å, and 10% when combining different spectral regions.

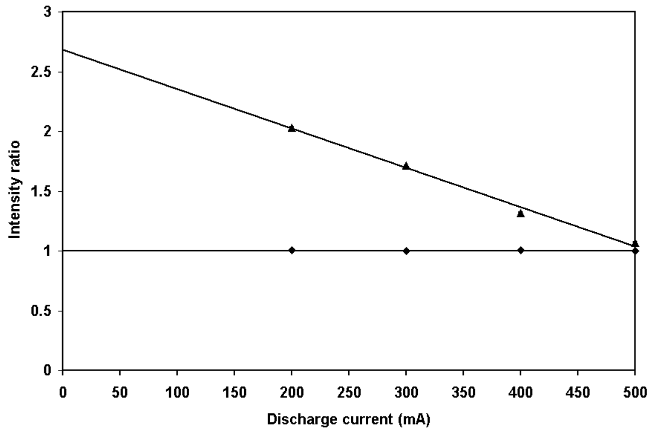

Fig. 1. Self absorption plot for three lines coming from the Th II level at 24 873.983 cm^{-1}. The tilted line shows the ratio between the intensities of the strongest line and the two weaker lines, while the horizontal curve shows the ratio between the two weak lines.

Strong lines involving the ground state are potentially affected by self absorbtion (SA). In order to check for this effect, the intensity ratio between different lines from the same upper level is plotted against the discharge current through the HC lamp. This is illustrated in Fig. 1, where the intensity relation between three lines coming from the Th II level at 24 873.893 cm^{-1} is plotted. Two of the lines are weak, $BF = 0.03$ and 0.01, respectively, while the third line is strong and involves the ground state. The strong line is clearly affected by SA, since the ratio between this line and the two weaker ones decreases at higher currents, while the ratio between the two weak lines is independent of the current. We adopted the ratio obtained by linear extrapolation to zero current.

3. Oscillator strengths

By combining the radiative lifetime (τ) and BFs one can derive transition probabilities (A-values) for lines from a particular level through the relation

$$A = \frac{BF}{\tau}\cdot \tag{1}$$

A-values can be converted to oscillator strengths or gf-values by

$$g_{\rm l}f = 1.4992 \times 10^{-16} \lambda^2 g_{\rm u} A, \tag{2}$$

where λ is in Å, A is in s^{-1}, and $g_{\rm u}$ and $g_{\rm l}$ are the statistical weights for the upper and lower levels, respectively.

The measured BFs, gf and log gf-values of the lines are reported in Table 2. Our log gf-values are also compared with the values of Corliss & Bozman (1962) and Corliss (1979). The total uncertainties in the gf–values reported in Table 2 are derived according to the method suggested by Sikström et al. (2001). The included contributions to the uncertainty come from: the intensity measurements, the intensity calibration, combining different

Table 2. Th II branching fractions (BFs) and gf-values. The lines are sorted by the upper level.

Upper level[a] (cm^{-1})	Lower level (cm^{-1})	λ_{air} (Å)	σ (cm^{-1})	BF	gf	log gf This work	log gf Corliss[b]	log gf C&B[c]	Unc. (% in gf)
18 214.426	8605.841	10 404.508	9754.074	0.03[d]	0.005	−2.311			51
$\tau = 376$ ns	1859.938	6112.837	16 354.488	0.25	0.015	−1.832		−2.942	40
$J = 1.5$	1521.896	5989.045	16 692.530	0.67	0.038	−1.414	−1.96	−2.641	10
	0.000	5488.629	18 214.426	0.05	0.002	−2.607		−3.304	13
19 050.829	9400.964	10 360.000	9649.865	0.06[d]	0.007	−2.143			49
$\tau = 579$ ns	4113.359	6692.726	14 937.470	0.08	0.004	−2.449		−3.420	15
$J = 1.5$	1859.938	5815.422	17 190.891	0.36	0.006	−1.901		−3.228	12
	0.000	5247.655	19 050.829	0.50	0.008	−1.846	−2.01	−2.662	11
19 248.270	10 855.323	11 911.506	8392.947	0.02[d]	0.005	−2.287			51
$\tau = 453$ ns	9711.962	10 483.366	9536.308	0.02[d]	0.004	−2.356			51
$J = 2.5$	8605.841	9393.774	10 642.429	0.004[d]	0.001	−3.158			51
	8460.352	9267.086	10 787.918	0.03[d]	0.006	−2.237			48
	7001.420	8163.120	12 246.850	0.05[d]	0.007	−2.149		−3.040	45
	4146.576	6619.945	15 101.694	0.18	0.015	−1.812		−2.933	11
	4113.359	6605.416	15 134.911	0.13	0.011	−1.953		−2.936	12
	1859.938	5749.388	17 388.332	0.12	0.010	−1.984		−3.020	11
	1521.896	5639.746	17 726.374	0.38	0.025	−1.605	−2.03	−2.677	11
	0.000	5193.826	19 248.270	0.07	0.004	−2.380		−3.027	12
20 686.146	10 855.323	10 169.301	9830.823	0.01[d]	0.002	−2.714			14
$\tau = 502$ ns	9711.962	9109.794	10 974.184	0.01[d]	0.001	−2.989			14
$J = 2.5$	9061.103	8599.756	11 625.043	0.02[d]	0.002	−2.648			20
	8460.352	8177.179	12 225.794	0.01[d]	0.001	−2.875			16
	7001.420	7305.404	13 684.726	0.10[d]	0.010	−2.023		−2.967	24
	4146.576	6044.433	16 539.570	0.21	0.014	−1.860		−2.875	11
	4113.359	6032.318	16 572.787	0.05	0.003	−2.532			12
	1859.938	5310.267	18 826.208	0.14	0.007	−2.149		−2.822	11
	1521.896	5216.597	19 164.250	0.19	0.009	−2.039		−2.470	11
	0.000	4832.803	20 686.146	0.27	0.011	−1.944		−2.734	11
21 131.799	13 250.508	12 684.806	7881.291	0.05[d]	0.004	−2.433			55
$\tau = 1290$ ns	9061.103	8282.250	12 070.696	0.05[d]	0.001	−2.840			55
$J = 1.5$	8605.841	7981.226	12 525.958	0.14[d]	0.004	−2.390		−3.140	50
	8018.192	7623.568	13 113.607	0.04[d]	0.001	−2.996			55
	7828.559	7514.896	13 303.240	0.04[d]	0.001	−3.003			55
	7001.420	7075.000	14 130.379	0.06[d]	0.001	−2.846			54
	6244.294	6715.188	14 887.505	0.08	0.002	−2.767			29
	4113.359	5874.351	17 018.440	0.10	0.002	−2.814			27
	1859.938	5187.468	19 271.861	0.11	0.001	−2.855			27
	1521.896	5098.043	19 609.903	0.29	0.004	−2.451		−2.724	27
	0.000	4730.881	21 131.799	0.05	0.001	−3.287			27
21 297.416	9711.962	8629.143	11 585.454	0.02[d]	0.003	−2.487			51
$\tau = 315$ ns	9400.964	8403.558	11 896.452	0.02[d]	0.005	−2.317			50
$J = 2.5$	8605.841	7877.075	12 691.575	0.02[d]	0.004	−2.443			50
	8460.352	7787.800	12 837.064	0.09[d]	0.016	−1.810		−2.574	12
	8018.192	7528.487	13 279.224	0.03[d]	0.004	−2.360			19
	7001.420	6993.037	14 295.996	0.19	0.027	−1.572		−2.611	11
	4113.359	5817.734	17 184.057	0.02	0.002	−2.785			12
	1859.938	5143.267	19 437.478	0.15	0.012	−1.933		−2.413	11
	1521.896	5055.347	19 775.520	0.16	0.012	−1.923		−2.484	11
	0.000	4694.092	21 297.416	0.30	0.019	−1.728		−2.364	11

Table 2. continued.

Upper level[a] (cm^{-1})	Lower level (cm^{-1})	$\lambda_{\rm air}$ (Å)	σ (cm^{-1})	BF	gf	log gf This work	log gf Corliss[b]	log gf C&B[c]	Unc. (% in gf)
21 682.747	10 855.323	9233.273	10 827.424	0.02[d]	0.003	−2.525			56
$\tau = 807$ ns	9400.964	8139.902	12 281.783	0.05[d]	0.005	−2.305		−3.047	54
$J = 3.5$	8605.841	7644.964	13 076.906	0.02[d]	0.002	−2.706			56
	6213.490	6462.648	15 469.257	0.36	0.022	−1.654			26
	4146.576	5700.917	17 536.171	0.53	0.026	−1.592		−2.240	25
	1521.896	4958.724	20 160.851	0.02	0.001	−3.227			26
22 642.105	10 379.122	8152.381	12 262.983	0.16[d]	0.005	−2.338		−2.927	49
$\tau = 3560$ ns	9711.962	7731.738	12 930.143	0.45[d]	0.011	−1.946		−2.695	27
$J = 4.5$	6213.490	6085.256	16 428.615	0.34	0.005	−2.272		−2.928	27
	4146.576	5405.209	18 495.529	0.04	0.001	−3.274			28
23 372.581	13 250.508	9876.691	10 122.073	0.004[d]	0.009	−2.044			54
$\tau = 81$ ns	12 219.976	8964.047	11 152.614	0.01[d]	0.004	−2.367			54
$J = 1.5$	9061.103	6985.472	14 311.478	0.02[d]	0.007	−2.151			53
	8605.841	6770.107	14 766.740	0.05	0.005	−2.269		−2.779	19
	8018.192	6510.997	15 354.389	0.02	0.004	−2.449			53
	4113.359	5190.872	19 259.222	0.09	0.009	−2.056		−2.426	19
	1521.896	4575.233	21 850.685	0.01	0.001	−3.076		−2.967	19
SA	0.000	4277.314	23 372.581	0.80	0.050	−1.301	−1.19	−1.696	7
24 132.035	14 349.388	10 219.381	9782.647	0.02[d]	0.010	−1.982			50
$\tau = 159$ ns	12 219.976	8392.541	11 912.068	0.02[d]	0.005	−2.305			51
$J = 1.5$	9061.103	6633.458	15 070.932	0.04[d]	0.008	−2.090			49
	8018.192	6204.128	16 113.843	0.04[d]	0.006	−2.208			50
	7828.559	6131.964	16 303.476	0.03	0.004	−2.387			32
	6244.294	5588.869	17 887.741	0.07	0.010	−1.995		−2.555	10
	4113.359	4993.942	20 018.676	0.01	0.001	−3.014			13
	0.000	4142.701	24 132.035	0.77	0.058	−1.239		−1.928	6
24 414.641	9061.103	6511.358	15 353.538	0.02	0.009	−2.038		−2.857	13
$\tau = 62.6$ ns	8605.841	6323.842	15 808.800	0.01	0.004	−2.434			51
$J = 1.5$	8460.352	6266.174	15 954.289	0.04	0.017	−1.767		−2.710	12
	8018.192	6097.194	16 396.449	0.01	0.005	−2.287			14
	7001.420	5741.170	17 413.221	0.04	0.015	−1.815		−2.587	12
	6244.294	5501.944	18 170.347	0.03	0.007	−2.129		−2.842	12
	4113.359	4924.422	20 301.282	0.03	0.008	−2.095		−2.651	12
SA	0.000	4094.747	24 414.641	0.81	0.130	−0.885	−0.99	−1.461	4
24 463.789	15 786.985	11 521.826	8676.804	0.01[d]	0.007	−2.147			51
$\tau = 95$ ns	15 236.637	10 834.612	9227.152	0.01[d]	0.006	−2.200			51
$J = 2.5$	12 219.976	8165.139	12 243.822	0.01[d]	0.005	−2.314			51
	10 855.323	7346.343	13 608.466	0.01[d]	0.007	−2.172		−2.840	51
	8605.841	6304.243	15 857.948	0.03	0.012	−1.934		−2.696	11
	8460.352	6246.930	16 003.437	0.01	0.003	−2.526			28
	8018.192	6078.972	16 445.597	0.01	0.004	−2.399			26
	7001.420	5725.012	17 462.369	0.02	0.007	−2.152			11
	4146.576	4920.561	20 317.213	0.02	0.004	−2.417			10
	4113.359	4912.529	20 350.430	0.08	0.018	−1.732		−2.461	10
	1859.938	4422.783	22 603.851	0.02	0.003	−2.549			10
	1521.896	4357.613	22 941.893	0.04	0.007	−2.173		−2.479	10
SA	0.000	4086.521	24 463.789	0.74	0.118	−0.929	−0.99	−1.458	6

Table 2. continued.

Upper level[a] (cm^{-1})	Lower level (cm^{-1})	λ_{air} (Å)	σ (cm^{-1})	BF	gf	log gf This work	log gf Corliss[b]	log gf C&B[c]	Unc. (% in gf)
24 873.983	8605.841	6145.283	16 268.142	0.004	0.006	−2.244			21
$\tau = 23.0$ ns	7001.420	5593.615	17 872.563	0.01	0.016	−1.782			21
$J = 2.5$	4146.576	4823.182	20 727.407	0.01	0.005	−2.313		−2.675	21
	1859.938	4343.951	23 014.045	0.01	0.011	−1.958		−2.173	21
	1521.896	4281.068	23 352.087	0.03	0.018	−1.746		−2.078	21
SA	0.000	4019.129	24 873.983	0.94	0.592	−0.228	−0.19	−0.651	3
25 188.120	15 236.637	10 045.999	9951.483	0.01[d]	0.003	−2.521			51
$\tau = 280$ ns	9400.964	6332.512	15 787.156	0.11	0.010	−2.012			12
$J = 1.5$	8018.192	5822.522	17 169.928	0.05	0.003	−2.482			12
	4113.359	4743.685	21 074.761	0.20	0.010	−2.019		−2.367	11
	1521.896	4224.241	23 666.224	0.20	0.008	−2.127		−2.430	11
	0.000	3969.003	25 188.120	0.43	0.015	−1.835		−2.407	11
25 440.231	15 786.985	10 356.371	9653.246	0.005[d]	0.007	−2.163			51
$\tau = 66$ ns	10 855.323	6854.511	14 584.908	0.01[d]	0.006	−2.205			51
$J = 2.5$	9400.964	6232.974	16 039.267	0.03	0.014	−1.865		−2.554	12
	9061.103	6103.641	16 379.128	0.02	0.011	−1.970			12
	8605.841	5938.576	16 834.390	0.02	0.011	−1.964			12
	7001.420	5421.836	18 438.811	0.03	0.011	−1.946		−2.536	11
	4146.576	4694.921	21 293.655	0.03	0.010	−1.998		−2.303	11
	1521.896	4179.715	23 918.335	0.20	0.047	−1.330		−1.756	11
SA	0.000	3929.669	25 440.231	0.66	0.138	−0.859	−1.03	−1.463	7
26 424.470	9711.962	5981.885	16 712.508	0.04	0.012	−1.920			49
$\tau = 140$ ns	9400.964	5872.603	17 023.506	0.07	0.019	−1.730			9
$J = 2.5$	4146.576	4487.496	22 277.894	0.40	0.045	−1.322		−1.899	8
	1859.938	4069.761	24 564.532	0.03	0.003	−2.572			9
	1521.896	4014.514	24 902.574	0.08	0.007	−2.131		−2.345	9
	0.000	3783.296	26 424.470	0.38	0.037	−1.436		−2.017	8
27 249.544	15 786.985	8721.660	11 462.559	0.04[d]	0.027	−1.525		−2.275	39
$\tau = 125$ ns	13 248.708	7140.462	14 000.836	0.04[d]	0.020	−1.659		−2.535	30
$J = 3.5$	12 570.493	6810.550	14 679.051	0.06[d]	0.024	−1.586		−2.393	28
	10 379.122	5925.892	16 870.422	0.16	0.058	−1.260		−2.198	8
	9711.962	5700.459	17 537.582	0.09	0.029	−1.570		−2.148	8
	8605.841	5362.250	18 643.703	0.02	0.006	−2.249			9
	6213.490	4752.414	21 036.054	0.49	0.114	−0.971		−1.619	6
	4146.576	4327.231	23 102.969	0.04	0.007	−2.152		−2.285	8
	4113.359	4321.019	23 136.185	0.01	0.002	−2.725			9
	1521.896	3885.768	25 727.648	0.04	0.007	−2.207		−2.287	8
28 243.812	9400.964	5305.577	18 842.848	0.01	0.023	−1.636		−2.35	14
$\tau = 11.5$ ns	9061.103	5211.577	19 182.709	0.002	0.003	−2.477			51
$J = 2.5$	8018.192	4942.844	20 225.620	0.003	0.006	−2.187			15
	7001.420	4706.251	21 242.392	0.02	0.032	−1.490		−2.18	12
	4146.576	4148.684	24 097.236	0.003	0.004	−2.387			15
	4113.359	4142.973	24 130.453	0.003	0.004	−2.429			15
	1859.938	3789.118	26 383.874	0.05	0.055	−1.259	−1.10	−1.60	11
SA	1521.896	3741.183	26 721.916	0.62	0.677	−0.170	−0.50	−1.00	8
SA	0.000	3539.587	28 243.812	0.29	0.287	−0.542	−0.86	−1.35	13

Table 2. continued.

Upper level[a] (cm^{-1})	Lower level (cm^{-1})	λ_{air} (Å)	σ (cm^{-1})	BF	gf	log gf This work	log gf Corliss[b]	log gf C&B[c]	Unc. (% in gf)
28 720.835	12 219.976	6058.610	16 500.868	0.01	0.015	−1.823			51
$\tau = 15.3$ ns	8605.841	4970.029	20 114.994	0.02	0.023	−1.647		−1.924	11
$J = 1.5$	7001.420	4602.886	21 719.415	0.03	0.027	−1.576		−1.973	11
	6244.294	4447.834	22 476.541	0.06	0.059	−1.232		−1.629	11
SA	1859.938	3721.825	26 860.897	0.61	0.406	−0.391	−0.69	−1.016	8
SA	1521.896	3675.567	27 198.939	0.27	0.177	−0.752	−0.75	−1.074	13
29 095.464	18 118.701	9107.654	10 976.763	0.01[d]	0.014	−1.871			51
$\tau = 28$ ns	12 570.493	6049.773	16 524.971	0.01	0.010	−1.991			50
$J = 2.5$	10 855.323	5480.863	18 240.141	0.01	0.013	−1.872			10
	9061.103	4990.032	20 034.361	0.01	0.008	−2.100			10
	8605.841	4879.156	20 489.623	0.01	0.008	−2.079			10
	8460.352	4844.755	20 635.112	0.02	0.012	−1.940			10
	7001.420	4524.838	22 094.044	0.03	0.021	−1.681		−2.001	9
	4146.576	4007.062	24 948.888	0.01	0.007	−2.153			10
	4113.359	4001.734	24 982.105	0.03	0.014	−1.865		−2.022	9
	1521.896	3625.628	27 573.568	0.28	0.112	−0.950	−0.99	−1.300	9
SA	0.000	3435.977	29 095.464	0.58	0.214	−0.670	−0.76	−1.075	6
30 972.162	9711.962	4702.309	21 260.200	0.01	0.014	−1.850		−2.146	8
$\tau = 15.5$ ns	8460.352	4440.866	22 511.810	0.11	0.120	−0.919		−1.251	8
$J = 2.5$	8018.192	4355.321	22 953.970	0.05	0.056	−1.253		−1.381	8
	4146.576	3726.724	26 825.586	0.11	0.088	−1.055		−1.283	8
	4113.359	3722.115	26 858.803	0.25	0.204	−0.691	−0.84	−1.096	8
SA	1859.938	3433.999	29 112.224	0.42	0.290	−0.537	−0.49	−0.741	8
	1521.896	3394.581	29 450.266	0.005	0.003	−2.497			17
	0.000	3227.774	30 972.162	0.04	0.025	−1.597		−1.771	9
31 353.125	8605.841	4394.895	22 747.284	0.04	0.030	−1.529		−1.434	10
$\tau = 8.8$ ns	7828.559	4249.679	23 524.566	0.04	0.026	−1.583		−1.667	10
$J = 1.5$	7001.420	4105.330	24 351.705	0.12	0.071	−1.148		−1.021	10
	4113.359	3670.058	27 239.766	0.05	0.030	−1.517		−1.150	10
	1859.938	3389.640	29 493.187	0.19	0.082	−1.088	−0.97	−1.211	9
SA	1521.896	3351.228	29 831.229	0.55	0.251	−0.600	−0.49	−0.726	7
	0.000	3188.553	31 353.125	0.01[d]	0.002	−2.627			51
32 957.429	9400.964	4243.924	23 556.465	0.02	0.063	−1.202		−1.283	12
$\tau = 6.5$ ns	9061.103	4183.565	23 896.326	0.02	0.048	−1.318		−1.491	10
$J = 3.5$	8605.841	4105.350	24 351.588	0.04	0.112	−0.949			10
	4146.576	3469.921	28 810.853	0.40	0.743	−0.129	−0.18	−0.361	9
	4113.359	3465.924	28 844.070	0.03	0.057	−1.246		−1.363	10
SA	1521.896	3180.194	31 435.533	0.49	1.064	+0.027	−0.36	−0.547	7

[a] SA indicates that the line has been corrected for self absorption.
[b] Values reported by Corliss (1979).
[c] Values reported by Corliss & Bozman (1962).
[d] Indicates that the line intensity is taken from Palmer & Engleman (1983).

spectral regions, the self absorption correction and the lifetime measurements. The uncertainty introduced by the fact that not all decay channels of a level can be observed (either because they are too weak or because they fall outside the covered wavelength interval), is not included but we have considered the residual BF due to such lines. Calculations with the Cowan code (Cowan 1981) were performed of the even configurations $6d^27s$, $6d7s^2$, $6d^3$, $5f^27s$, 5f7s7p and $5f^26d$, and the odd configurations $5f7s^2$, 5f6d7s, $5f6d^2$, 6d7s7p and $6d^27p$. In these calculations no

Table 3. Finding list for Th II transitions sorted by wavelength.

$\lambda_{\rm air}$ (Å)	Lower level (cm^{-1})	Upper level (cm^{-1})	log gf	Unc.[a]
3180.194	1521.896	32 957.429	+0.027	7
3188.553	0.000	31 353.125	−2.627	51
3227.774	0.000	30 972.162	−1.597	9
3351.228	1521.896	31 353.125	−0.600	7
3389.640	1859.938	31 353.125	−1.088	9
3394.581	1521.896	30 972.162	−2.497	17
3433.999	1859.938	30 972.162	−0.537	8
3435.977	0.000	29 095.464	−0.670	6
3465.924	4113.359	32 957.429	−1.246	10
3469.921	4146.576	32 957.429	−0.129	9
3539.587	0.000	28 243.812	−0.542	13
3625.628	1521.896	29 095.464	−0.950	9
3670.058	4113.359	31 353.125	−1.517	10
3675.567	1521.896	28 720.835	−0.840	13
3721.825	1859.938	28 720.835	−0.479	8
3722.115	4113.359	30 972.162	−0.691	8
3726.724	4146.576	30 972.162	−1.055	8
3741.183	1521.896	28 243.812	−0.170	8
3783.296	0.000	26 424.470	−1.436	8
3789.118	1859.938	28 243.812	−1.259	11
3885.768	1521.896	27 249.544	−2.207	8
3929.669	0.000	25 440.231	−0.859	7
3969.003	0.000	25 188.120	−1.835	11
4001.734	4113.359	29 095.464	−1.865	9
4007.062	4146.576	29 095.464	−2.153	10
4014.514	1521.896	26 424.470	−2.131	9
4019.129	0.000	24 873.983	−0.228	3
4069.761	1859.938	26 424.470	−2.572	9
4086.521	0.000	24 463.789	−0.929	6
4094.747	0.000	24 414.641	−0.885	4
4105.330	7001.420	31 353.125	−0.949	10
4105.350	8605.841	32 957.429	−1.074	10
4142.701	0.000	24 132.035	−1.239	6
4142.973	4113.359	28 243.812	−2.429	15
4148.684	4146.576	28 243.812	−2.387	15
4179.715	1521.896	25 440.231	−1.330	11
4183.565	9061.103	32 957.429	−1.318	10
4224.241	1521.896	25 188.120	−2.127	11
4243.924	9400.964	32 957.429	−1.202	12
4249.679	7828.559	31 353.125	−1.583	10
4277.314	0.000	23 372.581	−1.301	7
4281.068	1521.896	24 873.983	−1.746	21
4321.019	4113.359	27 249.544	−2.725	9
4327.231	4146.576	27 249.544	−2.152	8
4343.951	1859.938	24 873.983	−1.958	21
4355.321	8018.192	30 972.162	−1.253	8
4357.613	1521.896	24 463.789	−2.173	10
4394.895	8605.841	31 353.125	−1.529	10
4422.783	1859.938	24 463.789	−2.549	10
4440.866	8460.352	30 972.162	−0.919	8
4447.834	6244.294	28 720.835	−1.320	11
4487.496	4146.576	26 424.470	−1.322	8
4524.838	7001.420	29 095.464	−1.681	9
4575.233	1521.896	23 372.581	−3.076	19
4602.886	7001.420	28 720.835	−1.663	11
4694.092	0.000	21 297.416	−1.728	11
4694.921	4146.576	25 440.231	−1.998	11

Table 3. continued.

$\lambda_{\rm air}$ (Å)	Lower level (cm^{-1})	Upper level (cm^{-1})	log gf	Unc.[a]
4702.309	9711.962	30 972.162	−1.850	8
4706.251	7001.420	28 243.812	−1.490	12
4730.881	0.000	21 131.799	−3.287	27
4743.685	4113.359	25 188.120	−2.019	11
4752.414	6213.490	27 249.544	−0.971	6
4823.182	4146.576	24 873.983	−2.313	21
4832.803	0.000	20 686.146	−1.944	11
4844.755	8460.352	29 095.464	−1.940	10
4879.156	8605.841	29 095.464	−2.079	10
4912.529	4113.359	24 463.789	−1.732	10
4920.561	4146.576	24 463.789	−2.417	10
4924.422	4113.359	24 414.641	−2.095	12
4942.844	8018.192	28 243.812	−2.187	15
4958.724	1521.896	21 682.747	−3.227	26
4970.029	8605.841	28 720.835	−1.735	11
4990.032	9061.103	29 095.464	−2.100	10
4993.942	4113.359	24 132.035	−3.014	13
5055.347	1521.896	21 297.416	−1.923	11
5098.043	1521.896	21 131.799	−2.451	27
5143.267	1859.938	21 297.416	−1.933	11
5187.468	1859.938	21 131.799	−2.855	27
5190.872	4113.359	23 372.581	−2.056	19
5193.826	0.000	19 248.270	−2.380	12
5211.577	9061.103	28 243.812	−2.477	51
5216.597	1521.896	20 686.146	−2.039	11
5247.655	0.000	19 050.829	−1.846	11
5305.577	9400.964	28 243.812	−1.636	14
5310.267	1859.938	20 686.146	−2.149	11
5362.250	8605.841	27 249.544	−2.249	9
5405.209	4146.576	22 642.105	−3.274	28
5421.836	7001.420	25 440.231	−1.946	11
5480.863	10 855.323	29 095.464	−1.872	10
5488.629	0.000	18 214.426	−2.607	13
5501.944	6244.294	24 414.641	−2.129	12
5588.869	6244.294	24 132.035	−1.995	10
5593.615	7001.420	24 873.983	−1.782	21
5639.746	1521.896	19 248.270	−1.605	11
5700.459	9711.962	27 249.544	−1.570	8
5700.917	4146.576	21 682.747	−1.592	25
5725.012	7001.420	24 463.789	−2.152	11
5741.170	7001.420	24 414.641	−1.815	12
5749.388	1859.938	19 248.270	−1.984	11
5815.422	1859.938	19 050.829	−1.901	12
5817.734	4113.359	21 297.416	−2.785	12
5822.522	8018.192	25 188.120	−2.482	12
5872.603	9400.964	26 424.470	−1.730	9
5874.351	4113.359	21 131.799	−2.814	27
5925.892	10 379.122	27 249.544	−1.260	8
5938.576	8605.841	25 440.231	−1.964	12
5981.885	9711.962	26 424.470	−1.920	49
5989.045	1521.896	18 214.426	−1.414	10
6032.318	4113.359	20 686.146	−2.532	12
6044.433	4146.576	20 686.146	−1.860	11
6049.773	12 570.493	29 095.464	−1.991	50
6058.610	12 219.976	28 720.835	−1.911	51
6078.972	8018.192	24 463.789	−2.399	26
6085.256	6213.490	22 642.105	−2.272	27

Table 3. continued.

λ_{air} (Å)	Lower level (cm^{-1})	Upper level (cm^{-1})	log gf	Unc.[a]
6097.194	8018.192	24 414.641	−2.287	14
6103.641	9061.103	25 440.231	−1.970	12
6112.837	1859.938	18 214.426	−1.832	40
6131.964	7828.559	24 132.035	−2.387	32
6145.283	8605.841	24 873.983	−2.244	21
6204.128	8018.192	24 132.035	−2.208	50
6232.974	9400.964	25 440.231	−1.865	12
6246.930	8460.352	24 463.789	−2.526	28
6266.174	8460.352	24 414.641	−1.767	12
6304.243	8605.841	24 463.789	−1.934	11
6323.842	8605.841	24 414.641	−2.434	51
6332.512	9400.964	25 188.120	−2.012	12
6462.648	6213.490	21 682.747	−1.654	26
6510.997	8018.192	23 372.581	−2.449	53
6511.358	9061.103	24 414.641	−2.038	13
6605.416	4113.359	19 248.270	−1.953	12
6619.945	4146.576	19 248.270	−1.812	11
6633.458	9061.103	24 132.035	−2.090	49
6692.726	4113.359	19 050.829	−2.449	15
6715.188	6244.294	21 131.799	−2.767	29
6770.107	8605.841	23 372.581	−2.269	19
6810.550	12 570.493	27 249.544	−1.586	28
6854.511	10 855.323	25 440.231	−2.205	51
6985.472	9061.103	23 372.581	−2.151	53
6993.037	7001.420	21 297.416	−1.572	11
7075.000	7001.420	21 131.799	−2.846	54
7140.462	13 248.708	27 249.544	−1.659	30
7305.404	7001.420	20 686.146	−2.023	24
7346.343	10 855.323	24 463.789	−2.172	51
7514.896	7828.559	21 131.799	−3.003	55
7528.487	8018.192	21 297.416	−2.360	19
7623.568	8018.192	21 131.799	−2.996	55
7644.964	8605.841	21 682.747	−2.706	56
7731.738	9711.962	22 642.105	−1.946	27
7787.800	8460.352	21 297.416	−1.810	12
7877.075	8605.841	21 297.416	−2.443	50
7981.226	8605.841	21 131.799	−2.390	50
8139.902	9400.964	21 682.747	−2.305	54
8152.381	10 379.122	22 642.105	−2.338	49
8163.120	7001.420	19 248.270	−2.149	45
8165.139	12 219.976	24 463.789	−2.314	51
8177.179	8460.352	20 686.146	−2.875	16
8282.250	9061.103	21 131.799	−2.840	55
8392.541	12 219.976	24 132.035	−2.305	51
8403.558	9400.964	21 297.416	−2.317	50
8599.756	9061.103	20 686.146	−2.648	20
8629.143	9711.962	21 297.416	−2.487	51
8721.660	15 786.985	27 249.544	−1.525	39
8964.047	12 219.976	23 372.581	−2.367	54
9107.654	18 118.701	29 095.464	−1.871	51
9109.794	9711.962	20 686.146	−2.989	14
9233.273	10 855.323	21 682.747	−2.525	56
9267.086	8460.352	19 248.270	−2.237	48
9393.774	8605.841	19 248.270	−3.158	51
9876.691	13 250.508	23 372.581	−2.044	54
10 045.999	15 236.637	25 188.120	−2.521	51
10 169.301	10 855.323	20 686.146	−2.714	14
10 219.381	14 349.388	24 132.035	−1.982	50
10 356.371	15 786.985	25 440.231	−2.163	51
10 360.000	9400.964	19 050.829	−2.143	49
10 404.508	8605.841	18 214.426	−2.311	51
10 483.366	9711.962	19 248.270	−2.356	51
10 834.612	15 236.637	24 463.789	−2.200	51
11 521.826	15 786.985	24 463.789	−2.147	51
11 911.506	10 855.323	19 248.270	−2.287	51
12 684.806	13 250.508	21 131.799	−2.433	55

[a] Uncertainty in % in the f-value.

significant lines were predicted to fall outside the wavelength interval covered in the measurements. The residuals are therefore assumed to consist of lines too weak to be measured in the spectra. Since the branching ratio of the weakest lines measured is less than 1%, the residual BF contains lines weaker than this. The total residual BF is estimated to be small for levels with short lifetime. Table 3 is a finding list including all log gf-values reported in this paper sorted by wavelength.

4. Conclusion

In order to improve the quality of the atomic data used in cosmochronometers we have measured absolute oscillator strengths for 180 Th II lines by combining experimental values of branching fractions and radiative lifetimes.

The f-values obtained by this method can be used for a detailed abundance analysis of thorium in high-resolution spectra of stars enriched in heavy elements. The data will be applied to the metal poor star CS 31082-001, for which an age has been determined by using U II and Th II lines (Cayrel et al. 2001). The presence of thorium in this star is illustrated in Fig. 2. The stellar spectrum was obtained at the European Southern Observatory in Chile with the VLT telescope and UVES spectrograph. The resolving power is 70 000 and the signal to noise ratio is 150 at 3859 Å and 250 at 6000 Å.

With the present Th II data and simultaneously measured data for U II (Nilsson et al. 2001) it is now possible to make an improved determination of the age and decrease the uncertainty.

Acknowledgements. This work was supported by the Crafoord Foundation (HL), the Swedish National Space Board (SJ) and the Swedish Natural Science Research Council (SJ). We gratefully acknowledge the support from Prof. S. Svanberg and Lund Laser Centre. The authors would also like to thank Dr. V. Hill

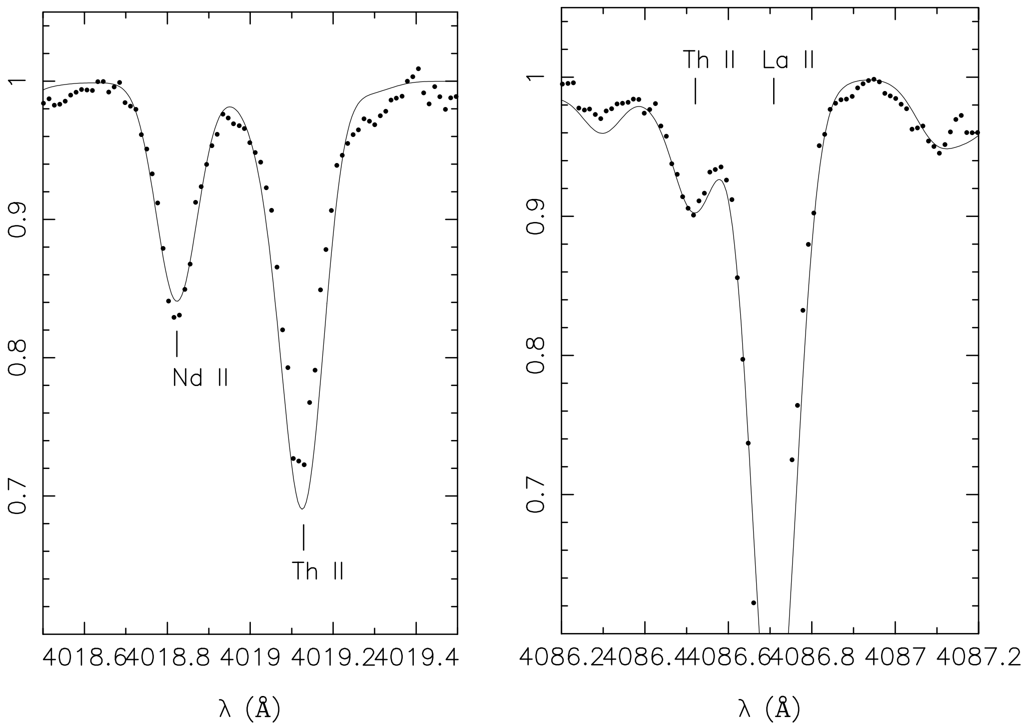

Fig. 2. Small spectral intervals including two of the strong Th II lines in the spectrum of CS 31082-001. The dotted line shows the recorded data points while the solid line shows a synthetic spectrum.

for preparing Fig. 2 and Prof. U. Litzén for his advice and assistance concerning the branching fraction measurements.

References

Andersen, T., & Petkov, A. P. 1975, A&A, 45, 237

Blaise, J., & Wyart, J. F. 1992, Energy levels and atomic spectra of actinides, International tables of selected constants, Publication subsidised by: The Frensh Centre National de la Recherche Scientifique and Belgian Government

Cayrel, R., Hill, V., Beers, T. C., et al. 2001, Nature, 409, 691

Corliss, C. H. 1979, MNRAS, 189, 607

Corliss, C. H., & Bozman, W. R. 1962, NBS monograph, vol. 53 (Washington, DC: US Govt Pritning Office)

Cowan, R. D. 1981, The Theory of Atomic Structure and Spectra (University of California Press, Berkeley 1981), The Cowan code is available at different Web sites, e.g. `http://plasma-gate.weismann.ac.il`, where a version modified for PC by Ralchenko and Kramida can be found

Li, Z. S., Lundberg, H., Wahlgren, G. M., & Sikström, C. M. 2000, Phys. Rev., A62, 032505

Nilsson, H., Ivarsson, S., Johansson, S., & Lundberg, H. 2001, A&A, submitted

Palmer, B. A., & Engleman, Jr. R. 1983, LA-9615, Los Alamos Internal Report

Sikström, C. M., Nilsson, H., Litzèn, U., Blom, A., & Lundberg, H. 2001, accepted by J. Quant. Spectrosc. Radiat. Transfer

Simonsen, H., Worm, T., Jessen, P., & Poulsen, O. 1988, Phys. Scr., 38, 370

Whaling, W., Carle, M. T., & Pitt, M. L. 1993, J. Quant. Spectrosc. Radiat. Transfer, 50, 7